Biochimica et Biophysica Acta 1818 (2012) 1656–1662

Contents lists available at SciVerse ScienceDirect

Biochimica et Biophysica Acta

journal homepage: www.elsevier.com/locate/bbamem

Probing membrane permeabilization by the antibiotic lipopeptaibol trichogin GA IV in a tethered bilayer lipid membrane

Lucia Becucci [a,*], Flavio Maran [b], Rolando Guidelli [a]

[a] Department of Chemistry, Florence University, Via della Lastruccia 3, 50019 Sesto Fiorentino (Firenze), Italy
[b] Department of Chemistry, University of Padova, Via Marzolo 1, 35131, Padova, Italy

ARTICLE INFO

Article history:
Received 31 January 2012
Received in revised form 16 March 2012
Accepted 30 March 2012
Available online 5 April 2012

Keywords:
Antimicrobial peptide
Ion channel
Tethered bilayer lipid membrane
Nucleation and growth

ABSTRACT

The lipopeptaibol trichogin GA IV (TCG) can be incorporated in the lipid bilayer moiety of a mercury-supported tethered bilayer lipid membrane (tBLM) at a non-physiological transmembrane potential of about −240 mV, negative on the trans side of the bilayer. Once incorporated in the tBLM, TCG is stable over the range of physiological transmembrane potentials and permeabilizes the membrane at transmembrane potentials negative of −80 ÷ −90 mV. The chronocoulometric behavior is consistent with a kinetics of nucleation and growth of bundles of TCG building blocks with ion-channel properties. The TCG building blocks also permeabilize the lipid bilayer, albeit at more negative transmembrane potentials, and can be tentatively regarded as dimers of aligned TCG helical monomers. The cyclic voltammograms of tBLMs incorporating TCG point to a voltage-gated behavior of the TCG channel, similar to that exhibited by the peptaibol alamethicin.

1. Introduction

Trichogin GA IV (TCG) is an amphipathic peptide that consists of a sequence of 10 amino acid residues with three nonproteogenic helicogenic α-aminoisobutyric acid (Aib) residues, the 1,2 amino alcohol leucinol at the C-terminus, and a lipophilic n-octanoyl group at the N-terminus. TCG belongs to the class of lipopeptide antibiotics [1–3], and has a remarkable capability of modifying membrane permeability [2–4]. Both TCG and its equally active analog TCG-OMe, in which leucinol is replaced by leucine methyl ester (Leu-OMe), have been extensively investigated. As distinct from the much longer peptaibol alamethicin, which is believed to form ion conducting barrel-stave aggregates [5,6], TCG is too short to span the whole membrane. The position and orientation of TCG and of its differently labeled analogs in model membranes have been studied using fluorescence spectroscopy [7,8], pulsed electron–electron double resonance (PELDOR) [9,10], and electron spin echo (ESE) [11]. The effect of TCG incorporation on the molecular properties of the membrane was investigated by multinuclear solid-state-NMR and FT-IR-absorption [12]. All these investigations concur in the conclusion that, at low peptide concentration, the helical TCG molecules lie just below the polar head region, parallel to the membrane surface [10,11,13]. The hydrophilic side of the helix, which includes the four Gly residues, is assumed to be turned toward the polar heads, with the hydrophobic side turned toward the hydrocarbon tails. On the basis of fluorescence spectroscopy experiments on giant unilamellar vesicles, Mazzuca et al. [8] showed that a fluorescent labeled TCG-OMe, when added on one side of the membrane, readily partitions on both sides. They also concluded that at relatively high TCG-OMe concentrations (≥3.5 μM) the peptide molecules are deeply inside the membrane, where they aggregate and determine membrane leakage and bioactivity. In other words, an increase in TCG-OMe concentration would trigger the passage from an inactive state, in which the peptide is near the polar head region, to a bioactive aggregation state embedded in the hydrocarbon tail region. Salnikov et al. [10] confirmed by PELDOR that an increase of the concentration of a spin labeled TCG-OMe derivative causes an orientation change resulting in the N-terminus of the peptide to be buried deeper inside the membrane; the most abundant aggregates were estimated to consist of peptide dimers with an antiparallel orientation. According to Syryamina et al. [11], at high peptide concentrations the three-pulse stimulated electron spin echo spectrum of spin labeled TCG-OMe provides evidence that two N-terminuses are mutually in close contact, rotating like a solid cylinder. It was concluded that the two head-to-head associated monomers are aligned along the direction of the surrounding lipid molecules, spanning the whole lipid bilayer. To explain the membrane leakage induced by TCG-OMe at high concentrations, it was postulated that these rotating dimers may promote translocation of polar molecules across the membrane by acting as a hole-drilling device.

All the above measurements, however, were carried out in the absence of an applied transmembrane potential $\Delta\phi_{lb}$. Moreover, all model membranes were prepared from well-defined lipid/peptide molar ratios, with the only exception of the work by Mazzuca et al. [8]. Different preset $\Delta\phi_{lb}$ values across large unilamellar vesicles were generated by Kropacheva and Raap [14], upon varying the K^+

* Corresponding author. Tel.: +39 055 457 3095; fax: +39 055 457 3385.
E-mail address: lucia.becucci@unifi.it (L. Becucci).

0005-2736/$ – see front matter © 2012 Elsevier B.V. All rights reserved.
doi:10.1016/j.bbamem.2012.03.021

concentration gradient across the vesicular membrane in the presence of the K^+-ionophore valinomycin. Dissipation of the transmembrane potential upon addition of TCG-OMe to the solution containing the vesicles (i.e., the cis side) was followed with two potential-sensitive dyes. The initial rate of $\Delta\phi_{lb}$ dissipation increases with an increase in the absolute value of the preset transmembrane potential when the latter is positive on the cis side, whereas it remains practically constant when the same potential is negative. Activation by imposing cis-positive transmembrane potentials, but not cis-negative ones, was also observed with other peptaibols, namely alamethicin and zervamicin. The observed power dependence of the ion diffusion rate k on TCG-OMe concentration ($k \propto [\text{TCG-OMe}]^N$ with $N \approx 3$–4) suggests that some aggregation is involved in ion permeation. In view of the moderately short chain of the peptide, it was hypothesized that a bundle of three or four TCG molecules, with the polar groups turned toward the interior of the bundle, may cage ions and shuttle them across the membrane in a valinomycin-like fashion [14]. However, the observation by Mazzuca et al. [8] that the activity of TCG-OMe is slightly higher in more rigid membranes, as opposed to the behavior of ion carriers, would disprove this hypothesis. Patch-clamp measurements in whole-cell configuration, using isolated photoreceptor rod outer segments incorporating TCG-OMe, did not lead to membrane permeabilization for $\Delta\phi_{lb}$ values ranging from −60 to +60 mV [15].

In this work, the behavior of TCG-OMe incorporated in a robust biomimetic membrane was investigated by cyclic voltammetry, chronocoulometry and electrochemical impedance spectroscopy. The biomimetic membrane was obtained by tethering a thiolipid monolayer to the surface of a hanging mercury drop electrode (HMDE). The thiolipid, 2,3-di-phytanyl-sn-glycerol-1-tetraethylene glycol-D,L-*a*-lipoic acid ester (DPTL) [16], consists of a tetraethyleneoxy hydrophilic chain, terminated at one end with a lipoic acid residue, for anchoring to the metal surface, and covalently linked at the other end to two phytanyl chains mimicking the hydrocarbon tails of a lipid. Self-assembling a phospholipid monolayer on top of the thiolipid monolayer gives rise to a lipid bilayer interposed between the aqueous solution and the hydrophilic chain (i.e., the "spacer"), which acts as an ionic reservoir. This mercury-supported tethered bilayer lipid membrane (tBLM) has been extensively employed for the investigation of ion channels [17].

2. Material and methods

Water was obtained by an inverted osmosis unit; it was then distilled once and redistilled from alkaline permanganate. Merck (Darmstadt, Germany) suprapur® KCl was baked at 500 °C before use to remove any organic impurities. Cholesterol (Chol), alamethicin and gramicidin A were purchased from Sigma-Aldrich (St. Louis, Missouri, U.S.A.) and used without further purification. Dioleoylphosphatidylcholine (DOPC) and diphytanoylphosphatidylcholine (DPhyPC) in chloroform solution and palmitoylsphingomyelin (PSM) in powder were purchased from Avanti Polar Lipids (Birmingham, AL, U.S.A.). TCG-OMe and its shorter omologue nOct-Aib-Gly-Gly-Leu-Aib-Gly-Ile-Leu-OMe were synthesized as described in the literature [18]. 2,3, di-O-phytanyl-sn-glycerol-1-tetraethylene-glycol-D,L-α lipoic acid ester lipid (DPTL) was provided by Prof. Adrian Schwan (Department of Chemistry, University of Guelph, Canada). Solutions of 0.2 mg/mL DPTL in ethanol were prepared from a 2 mg/mL solution of DPTL in ethanol. Stock solutions of this thiolipid were stored at −18 °C.

All measurements were carried out with a HMDE described elsewhere [19]. A home-made glass capillary with a finely tapered tip, about 1 mm outer diameter, was employed. Capillary and mercury reservoir were thermostated at 25 ± 0.1 °C in a water-jacketed box to avoid any change of the drop area due to temperature fluctuations. Mercury-supported tBLMs were obtained by tethering a DPTL monolayer on the HMDE; this was accomplished by keeping the mercury drop immersed in a 0.2 mg/mL DPTL solution in ethanol for 20 min. A monolayer consisting of DOPC, DPhyPC or a lipid mixture was then formed on top of the DPTL monolayer by spreading a lipid solution in pentane on the surface of a 0.1 M KCl aqueous solution. Immersion of the DPTL-coated mercury into the aqueous solution across the lipid film causes a lipid monolayer to self-assemble on top of the DPTL monolayer, thanks to the hydrophobic interactions between the alkyl chains of the phospholipid and those of the thiolipid. The tBLM was then subjected to repeated potential scans over a potential range from −0.200 to −1.200 V vs. Ag|AgCl|0.1 M KCl, while continuously monitoring the curve of the quadrature component of the current at 75 Hz against the applied potential using AC voltammetry, until a stable curve was attained.

Cyclic voltammetric, potential-step chronocoulometric and impedance spectroscopic measurements were carried out with an Autolab instrument PGSTAT12 (Echo Chemie, Utrecht, The Netherlands) supplied with FRA2 module for impedance measurements, SCAN-GEN scan generator and GPES 4.9007 software. Potentials were measured vs. a Ag|AgCl electrode immersed in a 0.1 M KCl working solution, and are referred to this electrode.

3. Results

The Hg-supported DPTL|lipid tBLM is a robust biomimetic membrane that is satisfactorily stable over the potential range from −0.200 to −1.200 V. TCG-OMe was incorporated into this biomimetic membrane from a 0.1 M KCl aqueous solution of this peptide. For the preparation of the distal lipid monolayer, DOPC, DPhyPC and a DOPC/PSM/Chol (45:44:11) mixture were alternatively employed. Incidentally, the DOPC/PSM/Chol mixture forms microdomains of a liquid-ordered phase rich in PSM and Chol (i.e., the lipid rafts), immersed in a liquid-disordered matrix rich in DOPC [20].

3.1. The electrochemical techniques used for the investigation of the tBLM

Potential-step chronocoulometry consists in subjecting the electrochemical system under investigation to a potential jump from an initial value E_i to a final value E_f and in recording the charge $Q(t)$ that flows as a consequence of this jump as a function of time. When applied to a Hg-supported DPTL|lipid tBLM in the absence of channel-forming peptides, the charge transient triggered by a potential jump is characterized by an initial flux of purely capacitive charge, lasting less than one millisecond; at sufficiently negative E_f values, this is followed by a linear increase of charge in time, due to a constant small reduction current, as schematically depicted in Fig. 1, curve *a*. This current, which is clearly visible only over a time scale of tens of seconds, is to be ascribed to a slight electroreduction of water to H_2, catalyzed by the sulfur atoms bound to the mercury surface [21]. Upon incorporating cation-selective or nonselective ion channels, either ohmic or voltage-gated, a potential jump from −0.300 V to a sufficiently negative final potential causes the channel to induce an ion flux into the tetraethyleneoxy (TEO) hydrophilic spacer. In particular, ohmic channels start moving ions into the TEO spacer in the proximity of a transmembrane potential, $\Delta\phi_{lb}$, equal to zero, while voltage-gated channels show this behavior only at some negative transmembrane potential. The ion flux is revealed by a negative charge that adds to the background charge recorded in the absence of channels. This negative charge is due to electrons that flow along the external circuit and accumulate on the metal surface, to maintain the electroneutrality of the whole electrified interface interposed between the bulk metal and the bulk aqueous solution. The electron charge density σ_M accumulating on the metal surface must be practically equal and opposite to the cation charge density accumulating in the hydrophilic spacer. In fact, the only other charge density located within the electrified interface is that present in the diffuse layer adjacent to the tBLM, which is much smaller than the other two [22]. As the final potential is made progressively more negative, an E_f value is ultimately attained at which the TEO spacer is completely saturated by the monovalent cations of the electrolyte. This gives rise to a charge step that adds to the background charge, with a

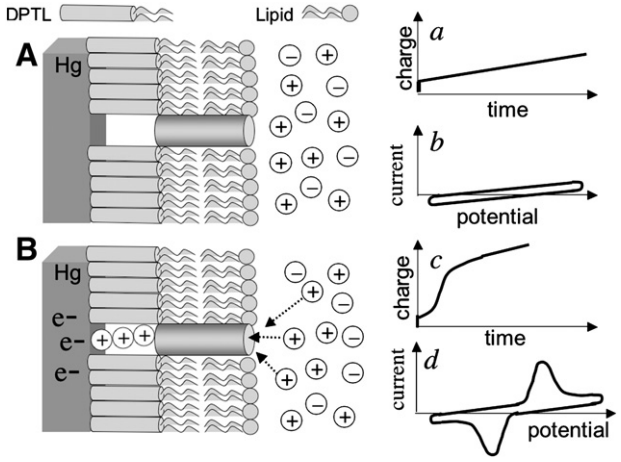

Fig. 1. Schematic picture of a tBLM incorporating an ion channel at a final applied potential, E_f', at which no cation flux takes place (A) and at a more negative final potential, E_f'', at which it takes place (B). Schematic plot of a charge transient following a negative potential jump from an initial potential E_i to the final potential E_f'' in the absence (*a*) and in the presence (*c*) of a voltage-gated channel, and schematic plot of a cyclic voltammogram covering the ($E_i > E > E_f''$) potential range in the absence (*b*) and in the presence (*d*) of an ohmic ion channel.

well-defined plateau and a height of about $-45 \div -50\ \mu C\ cm^{-2}$, as shown schematically in Fig. 1, curve *c*. This corresponds to the maximum charge of potassium ions that can be accommodated in the TEO spacer of the DPTL thiolipid, as verified for different ion channels, such as gramicidin [17e], melittin [17f], distinctin [17i] and alamethicin [17i]. With peptides that form ion channels by aggregation of helixes turning the hydrophilic side toward the lumen of the channel, these charge steps are often characterized by a sigmoidal shape. This shape has been explained on the basis of a general kinetic model that accounts for the potential-dependent penetration of adsorbed monomeric molecules into the lipid bilayer, followed by their aggregation with channel formation by a mechanism of nucleation and growth. The latter mechanism involves an induction period that is responsible for the sigmoidal shape. This behavior is exhibited by several peptides such as melittin [17f], monazomycin [17f], alamethicin [17i], distinctin [17i] and by small proteins such as sarcolipin [17d].

The cyclic voltammetric technique consists in scanning the applied potential at a constant scan rate from an initial to a final value and in then inverting the potential scan; this potential cycling can be repeated several times during a single experiment. The current is plotted versus the applied potential to yield the cyclic voltammetric trace. When applied to a Hg-supported DPTL|lipid tBLM in the absence of channel-forming peptides, the negative-going scan gives rise to a roughly constant negative capacitive current, due to a gradual accumulation of electrons on the metal surface and to a parallel accumulation of positive ions in the diffuse layer adjacent to the tBLM. The current also includes a resistive contribution due to a modest ion leakage through the lipid bilayer, which imparts a slight tilt to the current trace. The reverse scan yields a current with the same resistive contribution as that of the current generated by the negative-going scan, but with an opposite capacitive contribution with respect to the zero current axis. This results in a trace whose shape is similar to that of a tilted rectangle, as shown in Fig. 1, curve *b*. In the presence of an ion channel, the negative-going scan yields a negative current peak that adds to the background current, as soon as the appropriate transmembrane potential value is attained. This peak is due to cation influx into the spacer, and its integration over potential yields a charge of about $-45 \div -50\ \mu C\ cm^{-2}$, corresponding to spacer saturation. In the case of an ohmic ion channel, the reverse scan yields a positive current peak, roughly centrosymmetric with respect to negative current peak and with the inversion center located at an applied potential close to zero transmembrane potential, as shown in Fig. 1, curve *d*.

Electrochemical impedance spectroscopy consists in adding an a.c. voltage of given frequency to a constant potential E applied to the electrochemical cell, and in measuring the resulting current that flows at the same frequency. The amplitude of the a.c. voltage is of about 10 mV (peak-to-peak) to ensure a linear relationship between voltage and current. The frequency is varied by logarithmic steps from about 10^5 to 10^{-1} Hz. This frequency spectrum may allow a separation of the contributions from the different substructures composing the tBLM, on the basis of their different relaxation times. The response is usually interpreted by simulating the system by an "equivalent circuit" consisting of a series of RC meshes (i.e., parallel resistor and capacitor combinations), one mesh per each substructure. The relaxation time of a substructure is given by the product of the resistance R and the capacitance C of the corresponding RC mesh.

3.2. Potential-step chronocoulometric measurements

Chronocoulometric measurements were carried out by performing potential jumps from an initial potential $E_i = -0.300$ V to progressively more negative final potential values, E_f, and by recording the charge induced by the potential jump as a function of time, over a time window of 60 s. Each potential jump was preceded by an equilibration rest time of 30 s at E_i.

After stabilization of a tBLM incorporating TCG-OMe from its 1 μM solution by repeated potential cycles between −0.050 and −1.000 V, we carried out a series of potential jumps from E_i to final potentials E_f that were made progressively more negative by −50 mV increments. These jumps start yielding sigmoidal curves at $E_f = -0.700$ V, as shown in Fig. 2. As E_f becomes progressively more negative, the slope of the sigmoidal curve increases and its inflection point shifts gradually toward shorter times. The linear segment of these curves at longer times is sloping, due to a small constant current ascribable to a modest hydrogen evolution. Extrapolation of this linear segment to the $t = 0$ axis yields a charge of $-45 \div -50\ \mu C\ cm^{-2}$, corresponding to the ionic charge required to fill the hydrophilic spacer of the tBLM. In the presence of 5 μM TCG-OMe and over a time interval of 5 min, a sigmoidal curve is already observed at $E_f = -0.650$ V. Sigmoidal curves similar to those in Fig. 2 are also obtained with a constant initial potential $E_i = -0.550$ V. In this case, however, when proceeding toward progressively more negative E_f values, the height of the sigmoidal charge step starts decreasing with respect to its maximum value of $-45 \div -50\ \mu C\ cm^{-2}$; this is due to a rest time of 30 s at −0.550 V being insufficient to cause a complete expulsion of positive ions from

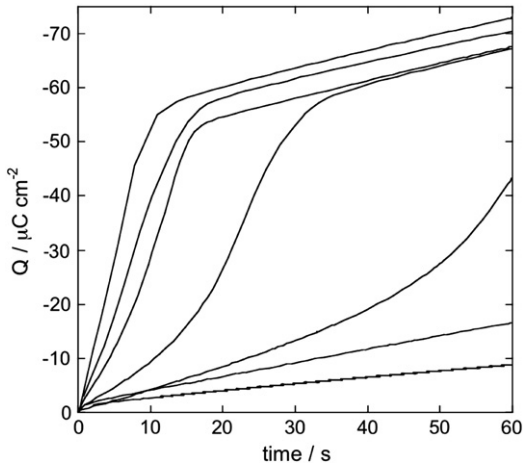

Fig. 2. Charge vs. time curves following potential jumps from $E_i = -0.300$ V to progressively more negative final potentials E_f at a DPTL|DOPC tBLM stabilized in aqueous 0.1 M KCl containing 1 μM TCG-OMe. Proceeding in the order of increasing height, the final potentials E_f are −0.600 V, −0.650 V, −0.700 V, −0.750 V, −0.800 V, −0.850 V and −0.900 V.

the hydrophilic spacer. The sigmoidal shape of the charge transients in Fig. 2 is indicative of a kinetic process of nucleation and growth of TCG-OMe building blocks with ion-channel formation, as shown on the basis of models [23,24]. These building blocks are expected to have the polar side, comprising primarily Gly residues, turned toward the lumen of the channel.

A chronocoulometric behavior similar to that exhibited by a tBLM incorporating TCG-OMe from its 1 μM aqueous solution was also shown by its shorter homologue (data not shown), but only at the much higher concentration of 18 μM.

Occasionally, after stabilization of the tBLM incorporating TCG-OMe by repeated potential cycles, the TCG-OMe molecules exhibit a particularly high permeabilizing activity, as revealed by cyclic voltammetry. In this case, the charge transients recorded during a series of potential jumps identical to that in Fig. 2 do not show sigmoidal shape (data not shown). This behavior suggests that the ion channels formed in this particular situation remain stable during the whole series of chronocoulometric potential jumps, in which the tBLM is kept 30 s at −0.300 V before each potential jump. Conversely, the sigmoidal shape shown in Fig. 2 indicates that each single potential jump is accompanied by nucleation and growth kinetics.

By carrying out a series of potential jumps from $E_i = -0.300$ V to progressively more negative potentials at a freshly prepared tBLM immersed in a 1 μM solution of TCG-OMe in aqueous 0.1 M KCl, an appreciable increase in charge with respect to that in the absence of TCG-OMe starts to be observed only at −0.900 V. This is shown by curve *b* in Fig. 3, whose concavity is turned toward the horizontal time axis. A subsequent potential jump from E_i to $E_f = -0.950$ V yields a charge transient in which a sigmoidal curve adds to an initial portion still exhibiting a downward concavity. A further potential jump to $E_f = -1.000$ V yields a steep sigmoidal curve, about $-50\ \mu C\ cm^{-2}$ high. With a TCG-OMe concentration of 5 μM, this sigmoidal charge transient is already observed at $E_f = -0.800$ V. The appreciable increase in charge with respect to the background charge observed at about −0.900 V is not accompanied by a sigmoidal shape. We can tentatively explain this behavior by assuming that ion-channel formation by nucleation and growth is preceded by a stage in which the incorporation of TCG-OMe monomers can induce an ionic flux into the TEO spacer without their aggregation. Since a single TCG-OMe monomer is too short to span a lipid bilayer, it is reasonable to regard the formation of dimers consisting of two aligned monomers as a prerequisite for their subsequent aggregation into ion channels. This conclusion is supported by the cyclic voltammetric behavior (see below).

3.3. Cyclic voltammetric measurements

The cyclic voltammetric behavior of tBLMs incorporating TCG-OMe was essentially the same with a DOPC or DPhyPC distal monolayer, whereas some differences were observed with a DOPC/PSM/Chol distal monolayer.

Cyclic voltammograms were obtained by scanning the applied potential between −0.200 and −0.050 V to −1.000 V. At a scan rate of $10\ mV\ s^{-1}$, the first negative-going potential scan at a freshly prepared tBLM incorporating TCG-OMe from aqueous solutions of concentrations ranging from 1 to 5 μM shows two partially overlapping negative current peaks at about −0.95 V ÷ −1.00 V (see Fig. 4). No negative peak is observed on a freshly prepared tBLM incorporating TCG-OMe if the voltage scan does not cover potentials more negative than −0.800 V. As distinct from the negative-going current, the positive-going current is relatively flat and exhibits a rounded hump at about −0.50 V, as shown in Fig. 4. Repeated scanning causes the two negative peaks to shift gradually toward less negative potentials and to merge eventually into a single current peak. Current stabilization is attained when the negative current peak is at −0.75 V ÷ −0.70 V using a DOPC or DPhyPC monolayer, and at about −0.60 V using a DOPC/PSM/Chol monolayer. This positive shift, recorded on the same mercury drop, is ascribed to a progressive incorporation of peptide molecules into the lipid bilayer of the tBLM and/or to a change of the orientation or degree of aggregation of TCG-OMe molecules already present in the lipid bilayer. An increase in the TCG-OMe concentration from 1 to 5 μM shifts the stabilized negative peak slightly in the positive direction. The stability of TCG-OMe ion channels is apparent not only from chronocoulometric measurements, but also from cyclic voltammetric measurements. Thus, a stabilized peak potential remains practically unaltered upon keeping the tBLM at an applied potential of −0.400 V for 1 h, even though TCG-OMe incorporation requires application of potentials more negative than −0.850 V.

Integration of the area under the negative peak (or peaks) yields a charge density σ_M on the metal of about $-45\ \mu C\ cm^{-2}$ at all scan rates from 5 to $50\ mV\ s^{-1}$ and at all peptide concentrations from 1 to 5 μM. This implies that the negative-going voltage scan fills the spacer completely with K^+ ions, while the positive-going one expels them from the spacer into the bulk aqueous phase, in order to maintain steady-state conditions. The charge involved in the positive-going scan cannot be accurately measured because of the flatness of the cyclic voltammogram at potentials positive of −0.60 V. Moreover, at

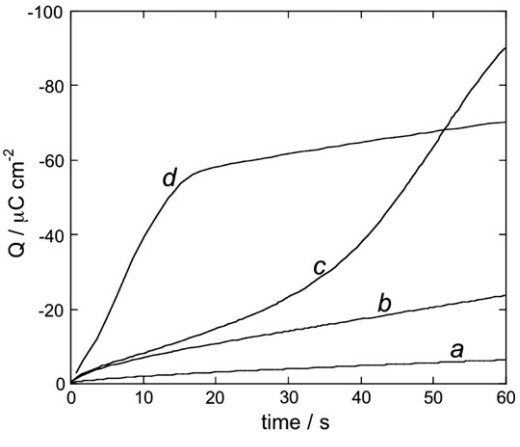

Fig. 3. Charge vs. time curves following potential jumps from $E_i = -0.300$ V to progressively more negative final potentials E_f at a freshly prepared DPTL|DOPC tBLM in aqueous 0.1 M KCl containing 1 μM TCG-OMe. The final potentials E_f are equal to −0.900 V (*b*), −0.950 V (*c*) and −1.000 V (*d*). Curve *a* was obtained at −0.900 V in the absence of TCG-OMe.

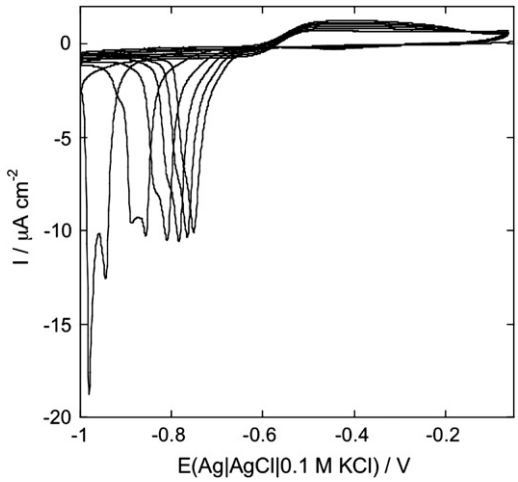

Fig. 4. Cyclic voltammograms of a freshly prepared DPTL|DOPC tBLM immersed in aqueous 0.1 M KCl containing 1 μM TCG-OMe. Proceeding from left to right, the cyclic voltammograms were obtained at a scan rate of $10\ mV\ s^{-1}$ after 1, 3, 6, 9, 12 and 15 cycles from the instant of the immersion.

these positive potentials, the current is positive with respect to the background capacitive current, as measured in the absence of the peptide, during both the positive-going scan and the negative-going one. The fact that a DOPC/PSM/Chol distal monolayer yields a stabilized negative peak more positive than that recorded with a DOPC or DPhyPC monolayer implies that the raft-forming lipid mixture favors the incorporation of TCG-OMe in the lipid bilayer. This is conceivably ascribable to the fatty acyl moiety of TCG-OMe. In fact, in mammalian membranes, which contain lipid rafts as distinct from microbial membranes, lipopeptides and lipidated proteins with long saturated acyl chains are sequestered into lipid rafts [25].

An increase of the scan rate from 10 to 200 mV s^{-1} causes the negative peak to split into two peaks, as shown in Fig. 5; while the less negative peak maintains a peak potential close to that of the single peak recorded at 10 mV s^{-1}, the more negative peak shifts markedly in the negative direction with an increase of the scan rate. This behavior can be explained by assuming again that the building blocks of the TCG-OMe channel may induce an ion flux across the lipid bilayer prior to their aggregation. At the low scan rate of 10 mV s^{-1}, all TCG-OMe dimers have sufficient time to aggregate with ion-channel formation, yielding a single peak. On the other hand, at higher scan rates not all dimers succeed in aggregating over the potential range of the single peak; the unclustered dimers will then induce an ion flux at more negative potentials, yielding the more negative voltammetric peak. This interpretation may also explain why the sigmoidal shape of the charge transients in Figs. 2 and 3 is less evident at the more negative final potentials. In fact, the abrupt jump to these potentials may well induce membrane permeabilization not only by ion channels, but also by single dimers. Evidence of a TCG-OMe dimer having two N-terminuses in close contact and rotating like a solid cylinder was recently provided by the three-pulse stimulated electron spin echo spectrum of spin labeled TCG-OMe [11]. The authors hypothesized that the rotational mobility of the dimer may promote transport of polar molecules in the membrane by acting like e hole-drilling device.

3.4. Electrochemical impedance spectroscopy measurements

These measurements were carried out over the frequency range from 0.1 to 10^5 Hz and by covering the potential range from −0.300 to −0.950 V by −50 mV increments. Impedance spectra are quite reproducible, but they show a critical potential at which an abrupt change in the electrical parameters prevents a satisfactory fitting, when using a single equivalent circuit throughout the whole potential range. Therefore, we will limit ourselves to showing the in-phase admittance Y' at 10 Hz, which is a rough measure of the tBLM conductivity, as a function of the applied potential E. On a freshly prepared tBLM in aqueous 0.5 μM TCG-OMe, Y' at 10 Hz starts to increase with respect to the background at −0.80 V, when proceeding in the negative direction (see Fig. 6). However, during the subsequent positive-going scan, Y' becomes vanishingly small only at −0.55 V. This confirms that a stable TCG-OMe incorporation in the membrane is favored by applying sufficiently negative potentials. The inset of Fig. 6 shows Y' vs. E plots at tBLMs in aqueous 1 μM TCG-OMe, recorded after stabilization by continuous voltage scans. The lipid forming the distal monolayer was either DPhyPC (solid circles) or the DOPC/PSM/Chol mixture (open circles). The potential at which TCG-OMe incorporation starts to increase the tBLM conductivity is more positive with the lipid mixture (−0.50 V) than with DPhyPC (−0.55 V), in agreement with cyclic voltammetric measurements. Both potentials are more positive than those at which cyclic voltammetry and chronocoulometry start sensing the effect of TCG-OMe incorporation; this is due to the higher sensitivity of impedance spectroscopy.

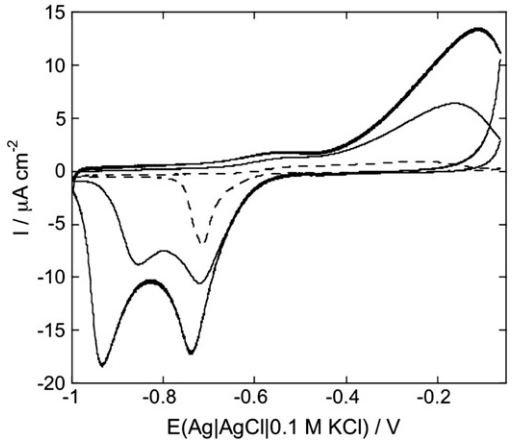

Fig. 5. Cyclic voltammograms of a DPTL|DOPC tBLM stabilized in aqueous 0.1 M KCl containing 1 μM TCG-OMe. In the order of increasing height, the scan rates are 10, 100 and 200 mV s^{-1}.

4. Discussion

The electric potential E can be related to the corresponding transmembrane potential $\Delta\phi_{lb}$, namely the potential difference across the lipid bilayer moiety of the tBLM. In the absence of ion channels in the lipid bilayer moiety, and hence in the absence of ions in the TEO spacer, $\Delta\phi_{lb}$ can be estimated from the equation $\Delta\phi_{lb} = 0.72 \times (E$ vs. Ag|AgCl|0.1 M KCl$) + 0.520$ V, derived on the basis of an approximate extra-thermodynamic procedure [26]. Thus, on a freshly prepared tBLM, the minimum negative value of $\Delta\phi_{lb}$ on the trans side of the membrane at which TCG-OMe starts to be incorporated amounts to about −240 mV, which is outside the range of physiological transmembrane potentials. Conversely, after incorporation, TCG-OMe permeabilizes the lipid bilayer stably at transmembrane potentials of $-80 \div -90$ mV, and its effect is measurable with electrochemical impedance spectroscopy even at $\Delta\phi_{lb} \cong -30$ mV. These are physiological transmembrane potentials, although their relatively high values suggest a voltage-gated behavior of TCG-OMe, analogous to that exhibited by the more widely known and much more extensively investigated peptaibol alamethicin [27,28]. In this connection, it should be noted that the cyclic voltammogram of alamethicin incorporated in the tBLM is similar to that of TCG-OMe, with a negative peak current and a relatively flat positive current (data not shown).

It is interesting to compare this behavior with that of the ohmic cation-selective gramicidin ion channel. Fig. 7 shows the cyclic voltammogram of a tBLM incorporating gramicidin from its 0.3 μM solution in aqueous 0.1 M KCl. On a freshly prepared tBLM the negative peak is at about −0.77 V while the positive one is at −0.475 V. Multiple voltammetric scans shift the negative peak in the positive direction while leaving the positive peak unchanged, until eventually the midpoint potential between the negative and positive peaks comes to practically coincide with the value, −0.520 V, corresponding to zero transmembrane potential. The shift of the negative peak is due to progressive gramicidin incorporation, which results in an increase in the rate of K^+ influx into the TEO spacer. On the other hand, the rate of K^+ exflux is unaffected by the amount of incorporated gramicidin. The shape of the negative peak is practically identical with that obtained from the positive peak by capsizing the positive half-plane on the negative one.

When compared with the cyclic voltammogram of the ohmic ion channel gramicidin, the highly asymmetric cyclic voltammogram of TCG-OMe can be regarded as typical of a voltage-gated channel, triggered by a trans-negative transmembrane potential. This behavior is well known in the case of the peptaibol alamethicin [27,28], which shares with TCG-OMe a non-symmetric cyclic-voltammetric behavior. The fact that the first negative-going scan at a freshly prepared tBLM in the presence of TCG-OMe does not give rise to any ionic influx into the TEO spacer for $E > -0.85$ V indicates that TCG-OMe is inactive over this potential range.

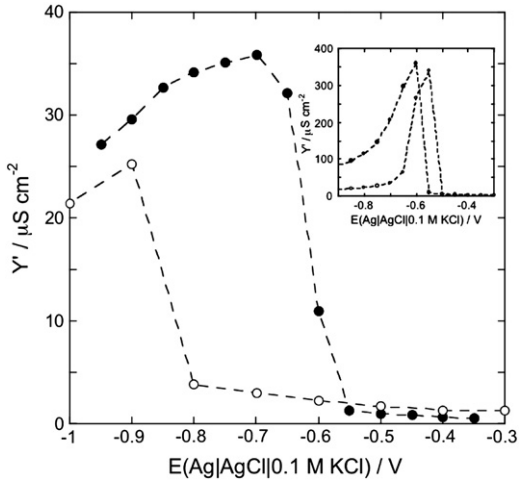

Fig. 6. Plots of the in-phase admittance Y' at 10 Hz against E at a DPTL|DOPC tBLM stabilized in aqueous 0.1 M KCl containing 0.5 μM TCG-OMe, as recorded during the negative-going scan (open circles) and during the subsequent positive-going scan (solid circles). The inset shows Y' vs. E plots at a DPTL|(DOPC/PSM/Chol) tBLM (open circles) and at a DPTL/DPhyPC tBLM (solid circles), both stabilized in aqueous 0.1 M KCl containing 1 μM TCG-OMe.

There is a general consensus [7–12] that this inactivity is associated with an orientation of the helical TCG-OMe molecules parallel to the membrane surface. After a single cyclic voltammogram between −0.05 and −1.00 V, a nonzero flat positive current is recorded, with the charge under this current necessarily equal and opposite to that under the negative current peak, to ensure steady-state conditions. This positive current is present even at potentials that are more positive than the potential at which TCG-OMe starts to be active during the first negative-going scan by 800 mV, although the ion flux is slower than at the negative potentials at which the negative peak is recorded. This indicates that the TCG-OMe helixes do not recover the original orientation parallel to the membrane surface, but assume some intermediate conformation allowing an ion flux, albeit slower than at negative potentials. It is also possible that they do not change conformation but exhibit sidedness within the lipid bilayer, such as to favor a higher ion flux in the negative direction than in the positive one. Overall, cyclic voltammetry thus appears to be a valuable tool for dynamic studies of ion channels in tBLMs.

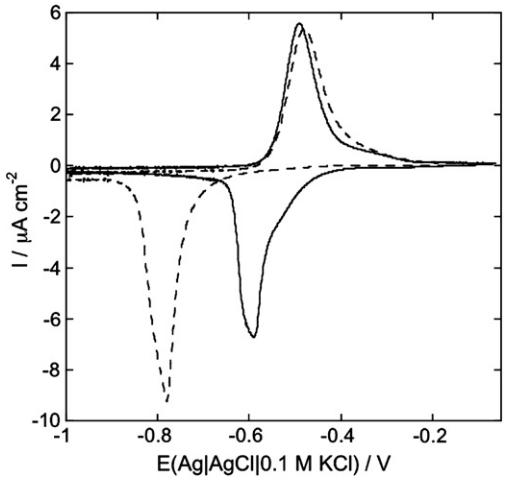

Fig. 7. Cyclic voltammograms of a DPTL|DOPC tBLM in aqueous 0.1 M KCl containing 0.3 μM gramicidin, at a scan rate of 10 mV s^{-1}, before (dashed curve) and after stabilization (solid curve).

5. Conclusions

The lipopeptaibol TCG-OMe can be incorporated in the lipid bilayer moiety of a mercury-supported tBLM at a non-physiological transmembrane potential of about −240 mV, negative on the trans side of the bilayer. However, we cannot exclude that a prolonged incubation of TCG-OMe in an aqueous solution bathing a conventional bilayer lipid membrane (BLM) may induce TGC-OMe incorporation in the membrane at physiological transmembrane potentials. Once incorporated in the tBLM, TCG-OMe is stable over the range of physiological transmembrane potentials and permeabilizes the membrane at transmembrane potentials negative of −80 ÷ −90 mV. The chronocoulometric behavior is consistent with a kinetics of nucleation and growth of bundles of TCG-OMe building blocks with ion-channel properties. Even these building blocks permeabilize the lipid bilayer, albeit at more negative transmembrane potentials, and can be tentatively regarded as dimers of aligned TCG-OMe helixes. The cyclic voltammograms of tBLMs incorporating TCG-OMe point to a voltage-gated behavior of the TCG-OMe ion channel, similar to that exhibited by the peptaibol alamethicin.

Acknowledgments

The financial support by the Regione Toscana (Nabla project) (L.B.), the Italian Ministero dell'Istruzione, dell'Università e della Ricerca (PRIN grant) and Fondazione Cariparo are gratefully acknowledged. Thanks are due to Dr. Ivan Guryanov (University of Padova) for the synthesis of TCG-OMe and its short analog.

References

[1] C. Auvin-Guette, S. Rebuffat, Y. Prigent, B. Bodo, Trichogin A IV, an 11-residue lipopeptaibol from *Trichoderma longibrachiatum*, J. Am. Chem. Soc. 114 (1992) 2170–2174.
[2] C. Toniolo, M. Crisma, F. Formaggio, C. Peggion, R.F. Epand, R.M. Epand, Lipopetaibols, a novel family of membrane active, antimicrobial petides, Cell. Mol. Life Sci. 58 (2001) 1179–1188.
[3] C. Peggion, F. Formaggio, M. Crisma, R.F. Epand, R.M. Epand, C. Toniolo, Trichogin: a paradigm for lipopeptaibols, J. Pept. Sci. 9 (2003) 679–689.
[4] S. Rebuffat, C. Goulard, B. Bodo, M.-F. Roquebert, The peptaibol antibiotics from *Trichoderma* soil fungi; structural diversity and membrane properties, Recent Res. Dev. Org. Biorg. Chem. 3 (1999) 65–91.
[5] R. Nagaraj, P. Balaram, Alamethicin, a transmembrane channel, Acc. Chem. Res. 14 (1981) 356–362.
[6] M.S.P. Sansom, The biophysics of peptide models of ion channels, Prog. Biophys. Mol. Biol. 55 (1991) 139–235.
[7] R.F. Epand, R.M. Epand, V. Monaco, S. Stoia, F. Formaggio, M. Crisma, C. Toniolo, The antimicrobial peptide trichogin and its interaction with phospholipid membranes, Eur. J. Biochem. 266 (1999) 1021–1028.
[8] C. Mazzuca, L. Stella, M. Venanzi, F. Formaggio, C. Toniolo, B. Pispisa, Mechanism of membrane activity of the antibiotic trichogin GA IV: a two-state transition controlled by peptide concentration, Biophys. J. 88 (2005) 3411–3421.
[9] A.D. Milov, D.A. Erilov, E.S. Salnikov, Yu.D. Tsvetkov, F. Formaggio, C. Toniolo, J. Raap, Structure and special distribution of the spin-labelled lipopeptide trichogin GA IV in a phospholipid membrane studied by pulsed electron–electron double resonance (PELDOR), Phys. Chem. Chem. Phys. 7 (2005) 1794–1799.
[10] E.S. Salnikov, D.A. Erilov, A.D. Milov, Yu.D. Tsvetkov, C. Peggion, F. Formaggio, C. Toniolo, J. Raap, S.A. Dzuba, Location and aggregation of the spin-labeled peptide trichogin GA IV in a phospholipid membrane as revealed by pulsed ERP, Biophys. J. 91 (2006) 1532–1540.
[11] V.N. Syryamina, N.P. Isaev, C. Peggion, F. Formaggio, C. Toniolo, J. Raap, S. Dzuba, Small-amplitude backbone motions of the spin-labeled lipopeptide trichogin GA IV in a lipid membrane as revealed by electron spin echo, J. Phys. Chem. B 114 (2010) 12277–12283.
[12] C. Heuber, F. Formaggio, C. Baldini, C. Toniolo, K. Müller, Multinuclear solid-state-NMR and FT-IR-absorption investigations on lipid/trichogin bilayers, Chem. Biodivers. 4 (2007) 1200–1218.
[13] G. Bocchinfuso, A. Palleschi, B. Orioni, G. Grande, F. Formaggio, C. Toniolo, Y. Park, K.-S. Hahm, L. Stella, Different mechanisms of action of antimicrobial peptides: insights from fluorescence spectroscopy experiments and molecular dynamics simulations, J. Pept. Sci. 15 (2009) 550–558.
[14] T.N. Kropacheva, J. Raap, Ion transport across a phospholipid membrane mediated by the peptide trichogin GA IV, Biochim. Biophys. Acta 1567 (2002) 193–203.
[15] N. Vedovato, G. Rispoli, A novel technique to study pore-forming peptides in a natural membrane, Eur. Biophys. J. 36 (2007) 771–778.

[16] S.M. Schiller, R. Naumann, K. Lovejoy, H. Kunz, W. Knoll, Archaea analogue thiolipids for tethered bilayer lipid membranes on ultrasmooth gold surfaces, Angew. Chem. Int. Ed Engl. 42 (2003) 208–211.
[17] L. Becucci, M.R. Moncelli, R. Naumann, R. Guidelli, Potassium ion transport by valinomycin across a Hg-supported lipid bilayer, J. Am. Chem. Soc. 127 (2005) 13316–13323;
(b) L. Becucci, R. Romero Léon, M.R. Moncelli, P. Rovero, R. Guidelli, Electrochemical investigation of melittin reconstituted into a mercury-supported lipid bilayer, Langmuir 22 (2006) 6644–6650;
(c) L. Becucci, M.R. Moncelli, R. Guidelli, Impedance spectroscopy of OmpF porin reconstituted into a Hg-supported lipid bilayer, Langmuir 22 (2006) 1341–1346;
(d) L. Becucci, R. Guidelli, C.B. Karim, D.D. Thomas, G. Veglia, An electrochemical investigation of sarcolipin reconstituted into a mercury-supported lipid bilayer, Biophys. J. 93 (2007) 2678–2687;
(e) L. Becucci, A. Santucci, R. Guidelli, Gramicidin conducting dimers in lipid bilayers are stabilized by single-file ionic flux along them, J. Phys. Chem. B 111 (2007) 9814–9820;
(f) L. Becucci, R. Guidelli, Kinetics of channel formation in bilayer lipid membranes (BLMs) and tethered BLMs: monazomycin and melittin, Langmuir 23 (2007) 5601–5608;
(g) L. Becucci, M.V. Carbone, T. Biagiotti, M. D'Amico, M. Olivotto, R. Guidelli, Incorporation of the HERG potassium channel in a mercury supported lipid bilayer, J. Phys. Chem. B 112 (2008) 1315–1319;
(h) L. Becucci, R. Guidelli, C.B. Karim, D.D. Thomas, G. Veglia, The role of sarcolipin and ATP in the transport of phosphate ion into the sarcoplasmic reticulum, Biophys. J. 97 (2009) 2693–2699;
(i) L. Becucci, M. Papini, D. Muller, A. Scaloni, G. Veglia, R. Guidelli, Probing membrane permeabilization by the antimicrobial peptide distinctin in mercury-supported biomimetic membranes, Biochim. Biophys. Acta 1808 (2011) 2745–2752.
[18] C. Toniolo, M. Crisma, F. Formaggio, C. Peggion, V. Monaco, C. Goulard, S. Rebuffat, B. Bodo, Effect of N^{α}-acyl chain length on the membrane-modifying properties of synthetic analogs of the lipopeptaibol trichogin GA IV, J. Am. Chem. Soc. 118 (1996) 4952–4958.
[19] M.R. Moncelli, L. Becucci, A novel model of the hanging mercury drop electrode, J. Electroanal. Chem. 433 (1997) 91–96.
[20] L. Becucci, S. Martinuzzi, E. Monetti, R. Mercatelli, F. Quercioli, D. Battistel, R. Guidelli, Electrochemical impedance spectroscopy and fluorescence lifetime imaging of lipid mixtures self-assembled on mercury, Soft Matter 6 (2010) 2733–2741;
(b) L. Becucci, F. Scaletti, R. Guidelli, Gel-phase microdomains and lipid rafts in monolayers affect the redox properties of ubiquinone-10, Biophys. J. 101 (2011) 134–143.
[21] S.G. Mairanovskii, Theory of catalytic hydrogen waves in organic polarography, Russ. Chem. Rev. 33 (1964) 38–55.
[22] L. Becucci, R. Guidelli, Equilibrium distribution of K^+ ions in the hydrophilic spacer of tethered bilayer lipid membranes, Soft Matter 5 (2009) 2294–2301.
[23] L. Becucci, M.R. Moncelli, R. Guidelli, Pore formation by 6-ketocholestanol in phospholipid monolayers and its interpretation by a general nucleation-and-growth model accounting for the sigmoidal shape of voltage — clamp curves of ion channels, J. Am. Chem. Soc. 125 (2003) 3785–3792.
[24] L. Becucci, R. Guidelli, Kinetics of channel formation in bilayer lipid membranes (BLMs) and tethered BLMs: monazomycin and melittin, Langmuir 23 (2007) 5601–5608.
[25] D.A. Brown, E. London, Structure and function of sphingolipid and cholesterol-rich membrane rafts, J. Biol. Chem. 275 (2000) 17221–17224.
[26] R. Guidelli, L. Becucci, Estimate of the potential difference across metal/water interfaces and across the lipid bilayer moiety of biomimetic membranes: an approach, Soft Matter 7 (2011) 2195–2201.
[27] M. Eisenberg, J.E. Hall, C.A. Mead, The nature of the voltage-dependent conductance induced by alamethicin in black lipid membranes, J. Membr. Biol. 14 (1973) 143–176.
[28] I. Vodyanoy, J.E. Hall, T.M. Balasubramanian, Alamethicin induced current voltage curve asymmetry in lipid bilayers, Biophys. J. 42 (1983) 71–82.